VOLUME 81 SEPARATE No. 696

PROCEEDINGS

AMERICAN SOCIETY
OF
CIVIL ENGINEERS

MAY, 1955

MODEL TESTS, ANALYTICAL COMPUTATION AND OBSERVATION OF AN ARCH DAM

by M. Rocha, J. Laginha Serafim, A.M. ASCE,
A. F. da Silveira, and J. M. Ressurreição Neto

POWER DIVISION

{Discussion open until September 1, 1955}

Copyright 1955 by the AMERICAN SOCIETY OF CIVIL ENGINEERS
Printed in the United States of America

Headquarters of the Society
33 W. 39th St.
New York 18, N. Y.

PRICE $0.50 PER COPY

THIS PAPER

--represents an effort by the Society to deliver technical data direct from the author to the reader with the greatest possible speed. To this end, it has had none of the usual editing required in more formal publication procedures.

Readers are invited to submit discussion applying to current papers. For this paper the final date on which a discussion should reach the Manager of Technical Publications appears on the front cover.

Those who are planning papers or discussions for "Proceedings" will expedite Division and Committee action measurably by first studying "Publication Procedure for Technical Papers" (Proceedings -- Separate No. 290). For free copies of this Separate--describing style, content, and format--address the Manager, Technical Publications, ASCE.

Reprints from this publication may be made on condition that the full title of paper, name of author, page reference, and date of publication by the Society are given.

The Society is not responsible for any statement made or opinion expressed in its publications.

This paper was published at 1745 S. State Street, Ann Arbor, Mich., by the American Society of Civil Engineers. Editorial and General Offices are at 33 West Thirty-ninth Street, New York 18, N. Y.

MODEL TESTS, ANALYTICAL COMPUTATION AND OBSERVATION OF AN ARCH DAM

M. Rocha,* J. Laginha Serafim,** A.M., ASCE
A. F. da Silveira*** and J. M. Ressurreição Neto***

INTRODUCTION

The Zezere-River hydroelectric scheme was started in 1947 by Hidro-Eléctrica do Zézere, with the erection of a dam at Castelo do Bode (1) designed by A. Coyne, Hon. M. ASCE. The project included a concrete arch upstream cofferdam (fig. 1,2) founded on crystalline shale. It is slightly unsymmetrical, of 34 m maximum height, and of about 140 m crown length, the ratio between length and height being therefore 4:1. The upstream face is a vertical cylindrical surface with a radius of 65 m, the downstream face being conical and concentric with the upstream face. The thickness ranges from 7 m at bottom to 2 m at the top.

The Laboratório Nacional de Engenharia Civil, in collaboration with Direcção Geral dos Serviços Hidráulicos (Board of Hydraulic Works) and with Hidro-Eléctrica do Zézere, outlined an extensive investigation, including model tests, trial-load analysis, calculation by the independent-arch theory and observation of the dam during the filling and emptying of the reservoir, which would provide information on the structural behavior of arch dams, and evaluate the usefulness of the analytical and experimental methods used in predicting this behavior. The investigations were started 1947, their experimental part being completed 1951.

Model tests were first carried out on a plaster-kiesel-guhr model. In this model a crack was induced by load at the base of the upstream face, and observation of the prototype showed that an analogous crack had actually developed in the dam.

To ascertain the effect of this crack upon the stress, use was made of a plastic (alkathene) model. On the plaster model, moreover, the effect of some horizontal cracks developed at the downstream face of the prototype, a little below the crown, upon filling of the reservoir was analysed (fig. 2). The upstream and downstream stresses were measured on both models, as well as the radial deflections of the downstream face. The tangential and vertical displacements were also measured on the plaster model.

Stress analysis by the trial-load method included radial adjustments only, but the unsymmetry of the structure was taken into account. A first approach having led to fairly high tensile stresses at the base of the cantilevers, a more accurate analysis was carried out on the assumption that the cantilevers cracked at the base.

*Acting Director, Nat. Civil Engineering Lab., Lisbon, Portugal.
**Head, Dams Studies Section, Nat. Civil Engineering Lab., Stuct. Branch, Lisbon, Portugal.
***Assistant Research Engineers, Nat. Civil Engineering Lab., Stuct. Branch, Lisbon, Portugal.

It was possible to carry out the test loading of the prototype when the temperatures of concrete, air and water were not very different, and when the loading-unloading cycle could be quickly made. Consequently, temperature changes were eliminated, and this afforded a simpler interpretation of the results.

The observation of the prototype included: measurement of strains at interior points by means of vibrating-wire meters, which also measured temperatures; measurement of deflections of the downstream face and of the crown by geodetic and slide target methods; measurement of joint opening; and measurement of angular displacements by clinometers.

The observation of the prototype was carried out after completion of much of the model tests and analytical computations. The cracks detected in the prototype entailed additional investigations, which could not be taken as far as desired, without too large an amount of work. Consequently this work does not correspond to the initially outlined program.

It was however considered worth while to publish the results arrived at, for very few opportunities have so far been available of comparing the actual and predicted behavior of arch dams.

The observation of real structures to check the stresses and deflections given by computations or model tests was attempted for the first time in the Stevenson Creek test dam,[2] in 1922.

Construction and proper testing of trial dams entail considerable difficulty and expenditure. On the other hand, on actual dams the effects of the different loadings, especially water pressure and temperature changes, can hardly be separated.

In Europe, especially in France,[3] vibrating-wire meters were developed and measurements of stresses in arch dams due to variations of hydrostatic pressure were made.

In the United States the good performance of the Carlson meters, together with a better knowledge of the properties of concrete, enabled further development by the Bureau of Reclamation, so the time-evolution of the stresses at nine points in the base of Shasta dam[4] was computed from readings. Reliable stress-measurements were also obtained by T.V.A. at Norris, Hiwassee[5] and Fontana[6] dams by Carlson meters. It should be noted, however, that in all those investigations no attempt was made to analyse the stresses by computation or model testing.

The remarkable investigations carried out on plaster and rubber models of Hoover dam[7] were compared with the results from thorough trial-load analysis. Nevertheless, no results of stress and displacement measurements for this dam have been so far available to the authors. Again, the results of the extensive model investigations of dams carried out in Italy and other European countries[8] have not been compared yet with those of prototype observations.

The results presented in this paper are those given by the very measurements, no correction whatsoever having been made such as might be required to allow for symmetry, continuity, or knowledge of the stress distribution in similar cases.

Model Investigations

Only the essential features of the investigations is presented here. A later detailed report will cover the whole series of model tests carried out at the Laboratory during the last 8 years. The methods so far used have already been published.[9] [10]

Models Tested

a) Plaster model - From the experience gained in model investigation of dams it was concluded that a mix of plaster and kieselguhr is the best material among those used.[7] [9]

The following are characteristics of this material: mechanical similarity, good workability, proper deformability, and low cost. It exhibits, however, too low a tensile strength; herein lies a serious drawback, for cracks may occur which are not easily detected. A further source of difficulty is the large extent to which the mechanical properties are affected by environmental moisture. Such influence can be considerably reduced if the outer surface of the models is waterproofed.

Taking into account the sensivity and size of the gages used in earlier tests, and the mechanical properties of the plaster-kieselguhr mix, the scale factor $\frac{1}{n} = \frac{1}{7\ 5}$ was selected for this model (fig. 3).

In casting the model, an accurate wooden mold was used, in order to give directly every detail of its final shape.

The section of the foundation ground reproduced in the model was given a thickness of 30 cm, i.e., roughly three times the maximum thickness of the dam model proper. The concrete tray used earlier for the model of Santa Luzia dam[11] was used again as the rigid base.

The model was made of a mixture of plaster and kieselguhr in the proportion of 2 to 1 by weight and water to produce a water-plaster ratio of 1.5 by weight. This water content gives a flowing mixture. The model was allowed to dry until moisture equilibrium was reached with the environment.

Application of hydrostatic pressure on the model was made by a properly shaped rubber bag filled with mercury. Thus the ratio between the specific gravity of the liquids loading the model and the prototype is G = 13,6.

The mechanical properties of the model material were determined by compression creep-tests on prisms cut from the model. The prisms were subjected to stresses of 2, 4, 6, 8 and 10 $kgcm^{-2}$, the strains being measured after 0, 2, 5, 10 and 20 min (fig. 4). The results show that the modulus of elasticity changes with time for stresses under 6 $kgcm^{-2}$, assuming the values indicated. The material may therefore be assumed to be perfectly elastic, for each loading time. A modulus of elasticity of 15,400 $kgcm^{-2}$ was adopted in evaluating model stresses, for strains and deflections were read after a 10 minutes loading, each reading taking not more than 1 1/2 minute. Poisson's ratio as given by tests was 0.20, no effect of creep having been measured.

The following similarity relations[11] hold between deflections δ_p, δ_m and stresses σ_p, σ_m respectively in the prototype and model:

$$\delta_p = \frac{E_m}{E_p} \frac{n^2}{G} \delta_m$$

$$\sigma_p = \frac{n}{G} \sigma_m,$$

wherein E_p, E_m stand for the moduli of elasticity of prototype and model respectively.

As will be seen later (section 6), a modulus of elasticity E_p = 260,000 $kgcm^{-2}$ was assumed for the concrete. Thus the similarity relations are

$$\delta_p = 24.5\ \delta_m$$

$$\sigma_p = 5.50\ \sigma_m$$

Despite of the crack caused by the tensile stresses at the upstream face, near the boundary line between dam and ground, it was decided to continue the tests.

At a later stage, some horizontal cracks were cut at the upper portion of the downstream face of the model, to bring about a closer replica of the prototype.

b) "Alkathene" model - In order to know the influence of the upstream crack at the base of the plaster model (which is very likely to develop in the prototype) it was decided to make another model which could be tested before and after cracking.

Since another plaster model could not be relied upon, a commercial synthetic resin was sought having a fairly good tensile strength, and conforming to the following requirements: ability to be cast without pressure or special molds, good workability, constant mechanical properties, and low modulus of elasticity, so that small models could be used. This led to the adoption of "alkathene" (I.C.I., England), a polyethylene resin. This material has the drawback of possessing a Poisson's ratio far above that of concrete, which could impair the similarity conditions. Molding is more complicated than for plaster, for it requires metallic molds, furthermore, a pouring temperature of 120° C and a very slow cooling are necessary.

The marked visco-elasticity of "alkathene" requires that considerable care be taken with regard to the time of loading the models. The high values of the coefficient of thermal expansion, about $200 \times 10^{-6}\ ^{o}C^{-1}$, together with the conspicuous influence of temperature on the mechanical properties, make it absolutely necessary that the tests be conducted in a temperature controlled room. If these precautions are taken, "alkathene" appears to be a very interesting material for model construction, because of its high tensile strength, toughness and nonfriability (whereby the handling becomes easier), and its absolute homogeneity.

The mechanical properties of "alkathene" were also determined by subjecting prisms to compressive creep tests at 22°C. The test results, illustrated by fig. 5, show that the modulus of elasticity changes with time. It was realized that the modulus of elasticity corresponding to any duration of loading changes with the temperature, according to the equation

$$E_\theta = E_{\theta_o}\left[1 - K(\theta - \theta_o)\right],$$

where K = 0,012. "Alkathene" can therefore be used for model studies as if it were a perfectly elastic material, provided that sufficient time is allowed between one test and the next, so that the influence of previous loading can be ignored.

Readings of strains and deflections were taken 5 min after loading; thus the value of 3,000 $kgcm^{-2}$ was adopted for the modulus of elasticity.

Owing to this low value and to the possibility of using short-base strain gages, the scale-factor $\frac{1}{n} = \frac{1}{200}$ was chosen for the "alkathene" model (fig. 6). Poisson's ratio as determined by creep tests was found to be 0.44. No change in this value with time was detected.

The model was subjected to a mercury load applied by a loading device as used for the plaster model.

The similarity relations holding for the deflections and the stresses are respectively

$$\delta_p = 33.9\ \delta_m$$

$$\sigma_p = \wedge 4.7\ \sigma_m \cdot$$

Measuring Instruments

a) Strain measurements - It was formerly intended to use vibrating-wire extensometers, as in testing the model of Santa Luzia dam,[11] but after the great advantage of electrical strain-gages was recognized, attempts were made to develop efficient techniques of fixing those gages onto the surface of plaster models.

A shellac coating applied to the model surface and infra-red dried for about half an hour was found to provide a proper base for fixing the Baldwin strain-gages. At the downstream face some additional strain measurements were made by Huggenberger extensometers, their results having been found to be in full agreement with those of the electrical strain gages. The latter have the advantage that they can be fixed quickly and used on the upstream face, where it is impossible to use mechanical extensometers if the pressure is applied by a liquid. It was found by tests that the direct influence of hydrostatic pressure on the extensometers can be neglected even for the highest pressure applied.

4-gage rosettes were first used and the four strains were always found to be in full agreement with one another, even when it was realized that the rosette had not been properly fixed. Such an agreement has always taken place, as the four gages are mounted on the same paper base. It was therefore decided to use, instead of rosettes, single extensometers located successively at each point, one horizontal, one vertical and one at 45°-angles to the others. The gages used had a 2 cm base. Readings were taken by a Baldwin "scanning recorder," enabling a recording of 48 gages in 1.5 minutes.

Since it was not found possible to fix the extensometers available onto "alkathene" surfaces, the tests of that model required that special gages be designed and made at the Laboratory. Those with a 1 cm base, consisted of electrical wire wound on a piece of thin cork and were fixed on the model surface by melting the "alkathene" (fig. 6). The gages were calibrated by fixing them to test prisms whose strains were also measured by means of mechanical and optical extensometers.

b) Deflection measurements - Deflections were measured in both models, at the downstream face only, by means of mechanical deflectometers (fig. 6 and 7) On the plaster model, radial, tangential and vertical displacements were measured. On the "alkathene" model, radial deflections only were measured, for its small dimensions made it too difficult to observe the other deflections.

Results of the Model Tests

a) Plaster-kieselguhr model - The model was tested under mercury levels at elevations 40, 50 and 55.

Elevation 55 lies 5 m above the crest of the prototype and it corresponds to a flood discharged over the dam. Of the results obtained only those relating to elevation 50 will be dealt with, since the prototype was not loaded above that elevation.

Figure 8 shows the points on each face at which strain measurements were made and the crack developed at the base of the upstream face, whose depth could not be determined.

As stated earlier, the analysis of the data from the prototype showed that it was desirable to reproduce horizontal cracks on the downstream face at the top of the model, as shown by fig. 8. After those cracks were provided in the model, strain measurements were made again in some points as shown in fig. 8.

The model was loaded successively as many times as required for taking 8 readings for each extensometer. The magnitude and direction of the strains were then determined from the average values by means of the corresponding Mohr's circles. The principal stresses were calculated by Hooke's law and transferred to the prototype by the similarity relations given. The pressure exerted by the mercury on the upstream face had to be taken into account in calculating the stresses at that face.

The magnitudes and directions of the stresses, as determined before and after reproducing the upper cracks, are shown in fig. 8. Taking account of the test conditions, the value of 2 $kgcm^{-2}$ was assigned as the upper limit of the error in the stress values.

Analysis of fig. 8 shows that the directions of the principal stresses at the upstream face near the foundation are approximately parallel to the foundation line, which is ascribed to the crack at the base. At the downstream face, the directions of the principal stresses have the usual distribution.

The downstream cracks decreased the compressive stresses at the crest. The decrease in the stiffness of the cantilevers also accounts for the increase in the vertical compressive stress which occurred on the upstream face of block DE el. 40, as well as for the decrease in the vertical tensile stress as observed on the downstream face of the same block at el. 32.

The results of the measurements of the radial, tangential and vertical deflections, on the model without downstream cracks, are presented in fig. 9, 10 and 11 respectively. In these figures are included the results from the "alkathene" model tests, prototype observations and trial-load analysis.

The maximum radial deflection of the plaster model (fig. 9) was found at the crest; its magnitude as transferred to the prototype is 1.6 cm. It should be noted that the maximum radial deflection generally occurs somewhat below the crest but this was not the case in the dam concerned, despite the unusual thickness of the crest (fig. 1).

The tangential deflections (fig. 10) range up to 0.5 cm and exhibit the usual distribution. They show a slightly unsymmetrical behavior of the structure. The vertical deflections (fig. 11), which could be detected at the crest only, reached a value of 0.3 cm.

b) "Alkathene" model - Seeing the small size of the model and the measuring instruments used, the accuracy of the results with this model was less than by the plaster model. The upper limit of the error in the stresses was estimated to be 3 $kgcm^{-2}$.

The model was first tested in the non-cracked condition. The stresses corresponding to a mercury load up to elevation 50 are presented in fig. 12.

To reproduce the base crack, a rather deep cut was made as shown by fig. 13. Here the stresses corresponding to the mercury load to elevation 50 are also shown.

By comparing fig. 12 to fig. 13 it is concluded that the cut, despite its depth, did not affect the stress distribution extensively. At the crest no influence could be detected. Other model tests confirm that an upstream crack near the base of an arch dam has very little influence upon the stress distribution, even for downstream face points at the same level as the crack.

As a result of the cut an increase in both vertical and horizontal compressive stresses was found to occur at the upstream face between el. 30 and el. 40, i.e., at the middle part. The maximum compressive stress increased from 24 to 29 $kgcm^{-2}$.

At the lower part of the downstream face there is also some stress increase, whose maximum is at el. 20, near the foundation. There the maximum compressive stresses increased by not more than 6 $kgcm^{-2}$, despite the cut in the neighborhood. At the base of the downstream face the cut was found to cause a slight decrease in both compressive stresses. Such a decrease does not appear possible; thus, on account of the accuracy of these tests the conclusion is drawn that there is practically no change in the stresses.

The increase in the vertical stresses at both faces of the crown (DE block) at the middle part should be noted, this being due to the restraint decrease at the base of the cantilevers.

At its lower upstream part the crackless model exhibits rather high tensile stresses up to 25 $kgcm^{-2}$. The compressive stresses due to the dead weight of the prototype (section 5) is only 10 $kgcm^{-2}$. The prototype would therefore be subjected to a tensile stress of 15 $kgcm^{-2}$ which could cause an upstream crack at the base.

Comparison of the stresses as determined by the plaster model and the "alkathene" model leads, as a rule, to fairly good agreement, except for downstream points near the right abutment. Such deviations are ascribed to a faulty bond at the abutment of the plaster model, which had been molded in two steps to simplify the construction.

The agreement referred to shows that, if account is taken of the accuracy of the measurements, Poisson's ratio can be regarded as not having significant influences. The "alkathene" model generally exhibited higher values of the second principal stresses near the foundation, especially at its lower part, those stresses being compressive on the downstream face and tensile on the upstream face (model in non-cracked condition). Such deviations are probably due to the high Poisson's ratio of "alkathene," whose effect becomes more important at the foundation.

The radial deflections were measured on the model before and after making the upstream cut at the base. The results corresponding to the latter case are presented in fig. 9. The crest deflections are not much affected by the cut at the base, which confirms the similar results concerning the stresses. As anticipated, the cut brought about an increase in the deflections below the crest.

Analytical Computations

To determine the stresses and displacements analytically both trial-load and independent-arch theories were used.

In the trial-load analysis only the radial displacements were considered and the modulus of elasticity of the foundation was assumed the same as that of the dam. Only the hydrostatic pressure was considered, for no other load is applied to the model nor acted upon the prototype during observation.

The trial-load analysis was carried out according to the U. S. Bureau of Reclamation procedure.[12] Four arches and six cantilevers were considered, as shown in fig. 14. As the arch at el. 50 was assumed to have the thickness of the crest, i.e., 3,25 m (fig. 1), no allowance for the changing thickness of the arches was made in the calculations. Likewise, the cantilever C_1

disregards the thickness of the right abutment (fig. 1) and, on the other hand, only the thickness of the left abutment is considered in the cantilever C_6.

A more accurate trial-load analysis would have been possible by increasing the number of arches and cantilevers with a considerable amount of additional calculation work. The arches and cantilevers were chosen to allow for the unsymmetrical features of the dam.

At an earlier stage of the model studies a stress analysis was carried out for the dam in a non-cracked condition, but the shape then selected for the abutment profile was not the one later adopted. Thus, the results of the former analysis are omitted.

That analysis showed a vertical tensile stress of 38 $kgcm^{-2}$ at the heel of the dam. This stress is supposed not to be much different from the one obtainable by considering the actual shape of the dam boundary. This magnitude accounts for the upstream crack developed in the plaster model and in the prototype.

The dam was then analysed assuming a crack at the base, with a depth of 3/4 the thickness at cantilever C_3 and half the thickness at cantilevers C_2 and C_4, the other cantilevers being considered uncracked.

This assumption does not really mean a true crack but a gradual changing in thickness of each cantilever between the decreased section and the next section considered in the analysis (at el. 20 for cantilever C_3 and el. 30 for cantilevers C_2 and C_4).

It should be noted that the highest stresses, shown in fig. 15, are developed at the base of the cracked cantilevers, with a peak of 104 $kgcm^{-2}$ at the crown cantilever. The stresses are much lower at the base of the non-cracked cantilevers.

The dead weight stresses were computed, as usual, by assuming the dam divided into independent blocks. The values obtained for the stresses at the crown cantilever C_3, are presented in Table I. If the crown cantilever is assumed to have a crack at the base of 3/4 of its thickness, the dead-weight stresses at the ends of the remaining plain section would have reached the values of -308 $kgcm^{-2}$ and +260 $kgcm^{-2}$ upstream and downstream respectively. This leads to the conclusion that the formation of so deep a crack in the prototype is not possible.

To compare results, the stresses were also computed by the method of independent arches. Figure 15 shows the values obtained for the abutment sections; they are far above those given by the trial-load analysis, especially on the downstream face.

The radial displacements, as determined on the assumption that the dam has an upstream crack, are presented in fig. 9. The distribution of these displacements is normal.

Observation of the Actual Structure

General

The cofferdam was constructed in blocks whose joints, A to J, are shown in fig. 1.

The concrete was placed in layers of 1.5 m thickness. Its cement content was 300 kg per cu. m and the coarse aggregate had a maximum size of 10 cm.

Since the cofferdam was an appurtenant work, and in view of the difficulties in its erection, the construction was not carried out so carefully as in the case of a permanent dam. The quality of the concrete was far from uniform,

the rate of concreting was rather irregular (some lifts were poured onto others about 1 year old), the concrete surfaces on which fresh concrete was to be placed were not carefully cleaned, the foundation rock was not grouted, and so on. In particular the joints were cement grouted without pressure, for no joint-seals had been provided.

A period of high inflow provided an opportunity of filling the reservoir, which impounded about 25 x 10^6 cu. m of water, in two days. On February 9th, 1950, at 2 p.m. (stage a), the gates at the diversion tunnel inlet were shut, and water started to be impounded. On February 11th, at 2 p.m. (stage b), the water level had reached el. 50. The gates were then opened on February 12th, at 10 a.m., the reservoir being completely emptied February 13th, at 5 p.m. (stage c).

The loading-unloading cycle thus took only 4 days. In addition, the mean air temperature happened to be practically unchanged and equal to those of the water and concrete during that period, an extremely favorable circumstance.

The instruments for measuring relative and absolute deflections, strains, joint-opening, and temperature were placed during and after the construction. Figure 16 shows their location. During the loading and unloading operations and for a further 4 days, readings were taken at every measuring instrument. The air and water temperatures were also recorded.

The properties of the concrete were found by testing 20 x 20 x 60 cm prismatic specimens cast during the construction, 32 cm ϕ concrete cores taken from the dam by drilling, and 45 x 45 x 90 cm prisms also taken from the dam. The average instantaneous modulus of elasticity as determined by testing the 20 x 20 x 60 prisms and the concrete cores was found to be 280,000 $kgcm^{-2}$. The prisms taken from the dam were subjected to creep tests which led to a modulus of elasticity of 260,000 $kgcm^{-2}$ corresponding to the time during which the prototype had been loaded. The latter value was used in interpreting the data. The average value of Poisson's ratio found by testing the prismatic specimens was 0.20.

Absolute Deflections

The absolute deflections were measured by the geodetic method[13] using a Wild T3 theodolite provided with a special centering device.

Figure 17 illustrates the plan which was followed to measure displacements likely to occur at stations I, II and III, from which the points on the downstream face shown in fig. 16 were sighted. On the crest of the dam two stations, IV and V, were erected from which it was possible to sight both the fixed points on the banks and stations I, II and III.

The absolute displacements produced at stages b and c, as determined by the geodetic method, are presented in fig. 18. The error of the displacements was kept lower than 0.2 mm. This high standard of accuracy was achieved by refinement in the techniques used.

The results presented in fig. 18 show that the dam did not recover its initial shape after unloading.

To secure a means of measuring promptly some absolute displacements during the loading-unloading cycle, station VI was erected on the right bank (fig. 17). From that station the components of the displacements along the directions at right angles to those passing through station VI, and through stations IV and V were measured. Fig. 19 illustrates the variation of those components during the tests, their magnitudes being plotted as a function of

the water elevation. Note the close agreement between the variation of the displacements at both points, and the non-reversible behavior of the dam, as shown by the geodetic measurements. The displacement of either station is 9 mm, and the displacements of stations IV and V as determined by the geodetic method are 7 mm and 10 mm respectively, which is regarded as a good agreement.

From fig. 18 the diagrams for radial and tangential displacements shown in fig. 9 and 10 were drawn up, and these will later (section 13) be compared to those predicted from model tests and analytical computations.

A high precision levelling was carried out for the points of the dam crest, and of the downstream foundation line (fig. 16). A Zeiss N3 level and invar sighting rods were used. The results obtained are collected in fig. 11, together with the vertical crest-deflections as given by the tests on the plaster model. The upward vertical deflections of the crest, which reached 0.5 cm, are not reversible. After unloading, the crest elevation remains higher than before loading.

The points near the foundation exhibit downward displacements during loading. After unloading they go back to their initial locations, with very small deviations. These displacements, about 0.2 cm, are probably due to the deflection undergone by the ground under the load of the impounded water. If, according to the knowledge of the nature of the strata, the value of 200,000 $kgcm^{-2}$ is assigned as the modulus of elasticity of the foundation, it is easily shown, by regarding the foundation as a semi-infinite body, that the maximum settlement is about 0.2 cm. The fact that the foundation remains free from residual deflections shows that the residual top deflection is probably due to the cracking of the horizontal construction joints, and to the uplift pressure exerted by water which percolated into the cracks, as shown in fig. 2.

Relative Displacements

The displacements of the dam relative to its foundations were determined from rotations measured by Huggenberger clinometers. These rotations were observed at the points indicated in fig. 16, which lie on a central section and on a section near the right abutment. The rotations on both radial and tangential vertical planes were measured at each point. The results of those measurements were in good agreement with those obtained by the geodetic method.

Joint Opening

The variation in joint opening was measured at the crest and the downstream face by a Huggenberger joint-meter.

The curves for the joint opening at the 14 points, and the water-level elevation and air-temperature curves are drawn in fig. 20. The minus values show that the joint edges approach each other. This was found at all the joints of the dam under the influence of the water load, and displacements of about 1 mm occurred at several points of the crest.

Some joints did not recover their initial opening after the reservoir had been emptied, which explains the residual deflections observed (fig. 18).

The curves of fig. 20 disclose, for the period of empty reservoir, a clear-cut influence of the air temperature upon the joint opening. A temperature rise brings about a decrease in joint-opening, and conversely.

When the prototype was under water load, leakage was found to occur through vertical joints and through joints between concrete lifts at the middle of the dam. The leakage through the vertical joints is easily understood, on the account of the grouting conditions.

Leakage through the horizontal joints was found to occur at that portion of the dam where model tests had detected tensile stresses up to 15 $kgcm^{-2}$; these stresses were not balanced by the dead weight, which produces compressive stresses up to 1 $kgcm^{-2}$ only.

Strains. Stress Computation

For measuring strains use was made of Coyne vibrating-wire strainmeters[14] located at the 16 points shown in fig. 16. At each point three strainmeters were placed along the sides of an equilateral triangle parallel to the faces of the dam and 50 cm away from them. At each elevation a control strain meter was placed to correct the readings taken at the strainmeters subjected to the dam stress. That strainmeter was embedded in a concrete prism which in turn was placed inside the dam concrete in such a way as to be unaffected by the surrounding stresses. The control strainmeters detect the length changes undergone by concrete under changing temperatures, moisture content, and the like. During the course of the tests, however, those meters detected only very small deviations, which shows that the volume changes of the concrete had been due to stresses alone.

At the points of the crest single horizontal strainmeters were used instead of triangle sets.

At some points on the downstream face, strain measurements were made by a Huggenberger joint-meter, but the results were of no significance, due to the large extent to which the strains in concrete near the face are affected by changes in air temperature.

Figure 21 shows the strain diagrams corresponding to some of the more representative strainmeter groups. The curves for water elevation, and air, water and concrete temperature are also plotted.

For the concrete temperature a stripe is marked whose boundaries correspond to the highest and lowest temperatures recorded at the different strain meters during each stage of loading.

The analysis of the strain diagrams is interesting. Some diagrams run like the water level one, whereas others exhibit abnormal runs, doubtless due to cracking.

Thus the crest strain meters 10u and 11d at first indicate compression, as expected, but strong disturbances are noticed in both meters after the water surface reaches el. 42. From this elevation on, the former indicates fairly constant strain, whereas the latter detects tensile stresses even before the water reaches its highest elevation.

Such behavior is understood if account is taken of the results of the plaster model test (fig. 8). As long as the downstream region of the model remains uncracked, compressive stress is induced there; as soon as cracks develop a stress-rearrangement takes place which produces a relief in upstream compression and gives rise to downstream tension. The behavior of meter 10u shows that, as expected, the cracks developed gradually as the water rose.

The strain meters of group 8u placed at 60^{o} angles to the horizontal also disclose a clear-cut influence of the downstream cracks, which became noticeable as the water reached el. 44. The horizontal meter exhibited a

normal behavior; this is also in full agreement with the observation of the plaster model, which had shown that the horizontal stress is not noticeably affected by the cracks (fig. 8).

The regularity exhibited by the meters of group 7d provides evidence of their not having been effected by the crack opening, which is due to their location.

Groups 5u and 6d exhibit disturbances as the water reaches el. 44, which is in agreement with the behavior of group 8u. Likewise, the upstream horizontal meter exhibits a regular behavior. The downstream one is affected by the cracks. As a rule the disturbances are not so strong as they are in group 8u; this probably means that the cracks were not so deep at el. 30 as they are at el. 40, where highest stresses tend to develop, as disclosed by both model tests and analytical computations.

In group 1u the 60^{o} sloping meter, which detects tension, exhibits some disturbance as soon as the water surface reaches el. 32, and, contrary to expectations, it shows no important length changes from el. 42 upwards. This may be due to the development of a tension crack in the base of the dam. In group 2d the 60^{o} sloping meter exhibits a regular behavior, which means that the upstream crack is probably not very deep.

After the dam was unloaded, all the strain meters of the two last mentioned groups disclosed noticeable tensile stresses which could not be properly accounted for. They are probably due to uneven foundation deformations.

Only two of the thirtysix strain meters embedded in the dam (belonging to groups 1u and 2d) were damaged.

The magnitudes and directions of the principal strains were then determined from the strains measured during stage b. The values used for that purpose in meter groups 1u and 2d were the average strains of loading and unloading. The principal stresses induced by a rise of the water up to el. 50 were computed assuming the concrete (section 6) to have a modulus of elasticity $E_p = 260{,}000$ kgcm^{-2} and a Poisson's ratio $\upsilon = 0{,}2$ (fig. 22).

Taking account of the way the observations were carried out, the value of 5×10^{-6} can be assigned as the upper limit of error in the strains, which are obtained as the differences between two readings of the instruments. It is concluded that the upper limit of error affecting the principal stresses is about 3 kgcm^{-2}. As the modulus of elasticity of the concrete may very often differ by 10% from the average used in the computations, it is estimated that the stresses will be affected by a further error of 10%. The errors to be expected are therefore about $3 + 3 = 6$ kgcm^{-2} for prototype stresses of the order of 30 kgcm^{-2}, $3 + 2 = 5$ kgcm^{-2} for stresses of the order of 20 kgcm^{-2}, and so on.

In Section 12 the stresses measured in the prototype and those given by model tests and analytical computations are compared. The interpretation of the results will be presented there. However, the sharp disagreement between the magnitide of the upstream tensile stress observed at the base of the dam, namely 9 kgcm^{-2}, and the value derived from the tests of the "alkathene" model, i.e., 25 kgcm^{-2} should now be pointed out. By considering the run of the strain diagram for that region (group 1u, fig. 21) and the compressive stress of 9 kgcm^{-2} induced by dead weight at the point under observation, it is concluded that the stresses due to hydrostatic pressure produced a crack which anulled the dead-weight compression. It cannot, however, be concluded that concrete did not withstand tensile stresses, for, in spite of these not having been detected by the strain diagram (fig. 21), they might have developed between two consecutive readings.

The agreement between the downstream vertical compressive stresses at the base of the prototype and the homologous ones derived from the "alkathene" model leads, on the other hand, to the conclusion that the crack concerned is probably not very deep; otherwise the considerable tension induced by the dead weight at that region of the prototype, as seen in Section 5, would have brought about a strong decrease in the compressive stress.

Structural Behavior of the Dam

The observation of the structure provided a judgment of the behavior of thin arch dams in wide valleys. The structural behavior was found to be satisfactory except for leakage, which occurred through both horizontal and vertical joints. Thin dams are bound to leak. In this case, however, such leakage could have been less had the construction been as careful as usual with actual dams.

It is believed that an entirely satisfactory behavior can be achieved for thin arch dams, provided the shape is designed to avoid high tensile stresses.

COMPARISON OF RESULTS

Comparative Analysis of the Stresses Observed at the Prototype, Derived from Model Tests and Determined by Computation

The stresses are compared only for those points observed in the prototype. As these points were 0.50 m from the dam faces, it was necessary to correct the values obtained from both model tests and analytical computations. Interpolation had also to be done for a few points, to obtain the values at the observed points of the prototype.

The results arrived at in this way are shown in Table II, in which the points are marked as in fig. 16 and 22. The results from the plaster model with downstream cracks are also included.

As far as the "alkathene" model is concerned, the magnitudes considered for evaluation were the average between the values obtained before and after upstream cracking. The reason was that the depth of the prototype crack was unknown, and that this crack has little influence at the points whose stresses are compared, except for point 1u.

In Table II the values corresponding to the trial-load analysis are those of the arch and cantilever stresses, without correction for those points at which the principal directions were not horizontal or vertical. The same applies to the values obtained by independent arches.

The differences from the values observed on the prototype and given by both model tests and analytical computations are listed in the last four columns of Table II.

In considering the comparison presented later it is necessary to bear in mind the errors which affect the various determinations. The differences between the corresponding prototype and model values amount up to 9 $kgcm^{-2}$, due only to the degree of accuracy of the measurements; the differences between prototype and analytical values may, similarly, amount to 6 $kgcm^{-2}$.

A short analysis of the stresses at the points mentioned in the Table follows.

Point 1u - The vertical tensile stress of 9 $kgcm^{-2}$ has already been ascribed to the development of an upstream crack at the base of the dam; that crack released the compressive stress due to dead weight (section 10).

Point 2d - There is close agreement between the two principal stresses as measured on the prototype and on the "alkathene" model (section 10).

Point 3u - For the highest stress there is a considerable difference between the values measured on the prototype and on the "alkathene" model. In so far as the observations of both models are concerned, this is the only difference which is not to be accounted for by the margin of error in the measurements or by the influence of cracks. The abnormal magnitude and direction of the principal stresses measured on the prototype, together with the agreement between the results of model and trial-load analysis, led to the conclusion that something occurred at this point of the prototype. Since it is a point near the foundation, it may be assumed that any disturbance was due to non-uniform rock deformation.

Point 4d - There is close agreement between prototype and both models in so far as the highest stress is concerned. On the other hand, analytical stress-analysis, mainly by independent arches, lead to values lying far above those given by other methods.

Point 5u - There is a fairly good agreement of all the values of the maximum compressive stress. Only the independent-arch theory leads to a considerably higher value.

Point 6d - Emphasis should be laid on the extent to which the downstream cracking of the plaster model improved the agreement between the values of the tensile stresses, as was to be expected. Similarly, the agreement between the lower compressive stresses at point 5u would also have been improved by observing the model after cracks had developed.

Points 7d and 8u - There is again a close agreement between the values of the higher stresses as measured on prototype and models. The values determined analytically are considerably higher.

Point 9d - The differences in the maximum-stress values, as found in both models, are slightly in excess of the probable errors of the measurements. To be particularly noted is the effect of the downstream cracks as observed on the plaster model, which justifies the second stress being a compressive one.

Points 10u and 11d - A remarkably close agreement is obtained by considering the influence of the downstream cracks. This accounts for the great differences as compared with the "alkathene" model and trial-load analysis.

Points 12u and 13d - There is agreement of the values determined by model tests and prototype observation, analytical methods having led to a rather higher value for point 13d.

Points 14u and 15d - All the values are found to agree fairly closely.

Point 16u - There is a fairly good agreement between prototype and model stresses, whereas the trial-load analysis gives a lower value for the highest stress.

From the foregoing the following general conclusions can be drawn.

Let us first consider the absolute values of the maximum principal stresses at each point. It is found that the differences between the prototype and both models can be accounted for, except for point 3u, by the margin of error; in other words, the structural behavior as predicted by model testing closely agrees with the actual behavior of the prototype. It should be particularly noted that point 3u, as well as point 9d, for which the differences encountered were a little too high, are located near the foundation, where disturbances are likely to occur.

The situation is quite different for the maximum stresses by the trial-load analysis. There are a number of points (4d, 6d, 7d, 8u, 13d, 16u) at which

considerably greater differences were found than are accounted for by the observation error. For point 8u, at which the highest prototype compressive stress, namely 29 $kgcm^{-2}$, was measured, the trial-load analysis gives slightly more than half, i.e., 16 $kgcm^{-2}$, whereas it gives about double the stress for point 7d.

Similar comparisons carried out have not, as a rule, disclosed such marked discrepancies. In this case the exceptional rigidity of the crown and the dissymetry of the dam must have contributed to these discrepancies.

Consideration of a larger number of arches and cantilevers, as well as of the tangential and twist adjustments would have given better results, but the amount of work entailed would have been infeasible in this case on the ground of both cost and time.

Among the values given by the trial-load analysis, reference should be made to those at the base of the cantilevers which were assumed to be cracked (fig. 15). In fact, those values are far above those given by the "alkathene" model, especially for the crown cantilever (fig. 13). Other model tests have shown that such a gradual thickness-change, as considered in the trial-load analysis with cracked cantilevers, entails a significant rearrangement of the stresses in the dam. But the actual stresses in the downstream portion of the cracked sections are not so high as those computed analytically.

The method of independent arches leads to much higher values, sometimes over twice as great as observed at the prototype at most points. An exception is the point of maximum compression, 8u, for which a lower stress is obtained by that method.

In so far as the minimum principal stresses, in absolute value, at each point are concerned, the model tests are found to give rather important discrepancies, especially if account is taken of the small magnitude of those stresses. The greatest discrepancies are observed, as they were in the case of the maximum stresses, at points in the vicinity of the foundation (4d and 7d). It is easily understood that the main effect of the irregular cracking of the rock may be a disturbance of the minimum principal stress, for its direction is roughly parallel to the foundation surface. The trial-load analysis also leads to unsatisfactory values of the minimum stresses.

Among the minimum principal stresses, the tensile ones are worth being noted. It was seen however that the errors affecting the measurements do not enable any conclusion to be drawn as to the extent to which models or analytical computations are dependable for that purpose.

Comparison of Deflections

The radial deflections observed at the prototype and in the model tests are presented in fig. 9, together with those computed by trial-load analysis.

At el. 30 and el. 40, the deflections observed at the prototype are rather larger than those given by both model tests and trial-load analysis. The situation is quite different at the crest, for the prototype deflections here are even smaller than those given by the plaster model. The large deflections at el. 30 and el. 40 are surely due to downstream horizontal cracks and to tightening of vertical joints (section 9). The horizontal cracks, which entail a decrease in cantilever effect, contributed to the decrease of the crest deflection.

The deflections given by the "alkathene" model were found to be smaller at every elevation. Moreover, the deflection diagrams exhibit different appearance near the abutments, at el. 40 and el. 50.

The tangential deflections measured at the prototype and at the plaster model (fig. 10), give reasonable agreement in their general appearance. The prototype gave higher values, which was surely due to the tightening of the vertical joints.

The vertical deflections at the prototype crest are rather larger than those obtained from the measurements on the plaster model (fig. 11). The reasons for this have been explained in section 7.

Summary and Conclusions

The most remarkable result achieved in these investigations is the evidence of close agreement between the values of the maximum principal stresses at each point as observed on the prototype and on both models (Section 12). On the other hand, the trial-load analysis led to stresses which are considerably different from those developed in the prototype, and the analytical method of independent arches gave results that are not to be accepted at all.

In view of the agreement between prototype and models it may be concluded that the dam as a whole behaved as a continuous solid body, despite extensive cracking and percolation of water through the cracks. This conclusion is regarded as very significant, for the observation of some similar structures could wrongly lead to the assumption that a dam behaves as a heap of concrete blocks rather than a continuous solid. Though the stress distribution may become irregular near the joints, such a lack of uniformity did not affect the stresses in the central portion of the blocks, in which the strain meters were located. Nor was any failure whatsoever observed near the joints, which would have occurred had there been important stress concentrations.

Emphasis is laid on the strong influence exerted by the horizontal downstream cracks on the state of stress at the crest. It was not until such cracks had been cut in one of the models that an agreement with the prototype could be achieved.

The tests carried out on one of the models, together with those carried out on models of other dams, enable the conclusion to be drawn that, contrary to the general assumption, an upstream crack in the base of the dam does not sensibly change the state of stress, even though it affects an important part of the dam thickness. This conclusion should be borne in mind when judging the tensile stresses computed in most cases at the upstream portion of the base, even if compression due to dead weight is taken into consideration.

In so far as the minimum principal stresses are concerned, no conclusion could be drawn on the suitability of model tests or analytical methods, for the accuracy of the measurements was not sufficient in view of the smallness of those stresses.

With regard to the maximum as well as the minimum principal stresses, the more significant differences between prototype and model results were observed near the foundation, which discloses the influence of non-uniform deformation and cracking of the rock. Those disturbances are more significant for thin arch structures.

The agreement between the prototype and model deflections was found to be less close than between the stresses. The deflections are evidently more affected by vertical-joint opening, cracking, and foundation conditions, than are stresses.

The more important problems in the technique of model testing are the selection of materials and the measurement of deformations.

As far as the materials are concerned, the experience gained in the attempts to improve the procedures leads to the conclusion that plaster-kieselguhr mixes are best suited (section 2). They have, however, the drawback of too low a tensile strength, which makes them less suitable when high tensile stresses are expected to develop.

"Alkathene," as well as other plastics used for model construction, have not that drawback, but the influence of its high Poisson's ratio, which changes from one case to another, is not yet well studied.

The electrical strain gages are best suited for measuring model deformations.

The observation of the prototype provided evidence of the high standard achieved in measuring deformations and deflections. This is clearly seen from the appearance of the diagrams for the strains as a function of the height of the reservoir (fig. 21), from the deflections along the dam (fig. 18), and so on.

The behavior of the dam under load was satisfactory, except for leakage, which would not have occurred had the dam been carefully built and the shape designed to avoid considerable tension. The cracks reveal that it would have been possible to save concrete.

Seeing the high standard achieved in model testing, in accuracy, in rapidity and in economy, it is stated that, except for minor projects, model studies should be carried out. The trial-load analysis can be used, in principle, with any shape and conditions of foundation. However, the necessity for reducing costs and time requires simplifications in the number of arches and cantilevers and adjustments, which leads to results of unknown accuracy, especially with dams exhibiting dissymmetry, irregular foundation-lines, heterogeneous foundations, shape singularities such as cracks, bulky abutments, spillway openings, and the like.

The only way of securing dependable information on the practical use of the analytical methods will be by systematically comparing their results with observations of models and prototypes.

REFERENCES

1. Xerez, A. C., "Le Barrage et L'Usine Hydroelectrique de Castelo do Bode (Portugal)." La Technique des Travaux. Juillet, Août, 1951, Nos. 7, 8.
2. Arch Dam Investigation. American Society of Civil Engineers, May, 1928, Vol. I.
3. Trans. III Congress Large Dams, Stockholm, 1948.

   Bellier J., Migny D., "Mesures Extensométriques du Barrage du Pas du Riot." Rapport 33.

   Nizery, A., "Mesures de Déformation Effectuées sur quelques Barrages Français." Rapport 34.

   Bourriot, R., "Rupture d'une Voûte d'Essai." Rapport 40.

   Hamon, "Mesures Extensométriques Effectuées sur le Barrage de Fabrèges lors de sa Mise en Eau." Rapport 42.

Bellier J., Blanchet, P., "Auscultation du Barrage du Gour Noir." Rapport 65.

4. Raphael, J. M., "The Development of Stresses in Shasta Dam." Trans. A.S.C.E., Vol. 118, pg. 289-321, 1953.

5. "Measurements of the Structural Behavior of Norris and Hiwasse Dams." Tennessee Valey Authority - T. M. No. 67, Knoxville, February, Aug., 1950.

6. "Measurements of the Structural Behavior of Fontana Dam." Tennessee Valey Authority T. M. No. 69. Knoxville, February, June, 1953.

7. "Model Tests of Boulder Dam." Boulder Canyon Project. Final Reports. Bureau of Reclamation, Bulletin 3. Denver, Colorado, 1939.

8. Oberti, G., "Ricerche Sperimentali sul Comportamento Statico delle Dighe." L'Elettrotecnica. Milano. Vol. XXXVI, No. 3, 1949.

Oberti, G., "Diga del Lumiei. Criteri di progetto e studi sperimentali." L'Energia Elettrica, Sept., 1948.

Jaeger, Ch., "Modern Trends in Arch Dam Investigation and Design. Civil Engineering and Public Works Review." Vol. 45, No. 541, pg. 572, 1950.

Tschech E., Jaburek, F., "Statische Modellversuche zu Gewölhestaumauern." Schweizeriche Bauzeitung, No. 16, pg. 215, 1951.

Nizery, A., Remenieras G. and Beaujoint N., "L'Étude sur Modèle Réduit des Contraintes dans les Barrages." Annales des Ponts et Chaussées. Juillet-Octobre, 1953.

9. Rocha, M., "Dimensionnement Experimental des Constructions." Annales de l'Institut Technique du Batiment et des Travaux Publics. No. 235, Février, 1952.

10. Rocha, M., "General Review of the Present Status of the Experimental Method of Structural Design." IV Congress International Ass. for Bridge and Structural Engineering, 1952.

11. Rocha, M., Serafim, J. L., "Model Tests of Santa Luzia Dam." Trans. III Congress Large Dams. C. 5. Stockholm, 1948.

12. "The Trial-load Method of Analysing Arch Dams." Boulder Canyon Project. Final Reports. Bureau of Reclamation, Bulletin 1. Denver, Colorado.

13. Rodrigues, O., "Mesures des Deplacements de Deuz Barrages Portugais par la Methode Trigonométrique." Trans. III Congress Large Dams. Report 64. Stockholm, 1948.

14. Coyne, A., "Quelques Résultats d'Auscultation Sonore." Annales de l'Institute Technique du Batiment et des Travaux Publics. Juillet-Août, 1948.

Mainstone, R. J., "Vibrating-Wire Strain Gauge for Use in Long-Term Tests on Structures." Engineering. London, 1953, No. 4566, pg. 154-156.

L'Hermite, R., "La Mesure de la Déformation des Solids." Circul. de l'Inst. Tech. du Bat. et des Travaux Publics, Paris, Série F, No. 37.

T A B L E I

STRESSES PRODUCED BY THE

DEAD WEIGHT AT THE CROWN CANTILEVER

Elevation m	Upstream face ($kgcm^{-2}$)	Downstream face ($kgcm^{-2}$)
40	3	1
30	6	1
20	8	1
15	10	2

TABLE II

COMPARISON OF THE STRESSES

Point	Stresses kgcm^{-2}						Deviations from the prototype values, kgcm^{-2}			
	Prototype	Model tests			Analytical computations		Model tests		Analytical computations	
		plaster	plaster, cracked	alkathene	trial-load	independent arches	plaster, cracked	alkathene	trial-load	independent arches
1 u	+9	-	-	+22 a)	+38 a)	-	-	-	-	-
	+2	-	-	+7 a)	-	-	-	-	-	-
2 d	-6	-	-	-5	-	-	-	-1	-	-
	-24	-	-	-22	-	-	-	-2	-	-
3 u	+1	-	-	+8	+3	-	-	-7	-2	-
	-13	-	-	-2	-6	-9	-	-11	-7	-4
4 d	+4	-3	-	-4	-3	-	+7 b)	+8	+7	-
	-17	-17	-	-16	-28	-38	0 b)	-1	+11	+21
5 u	-5	-11	-	-5	-7	-	+6 b)	0	+2	-
	-24	-25	-	-19	-23	-32	+1 b)	-5	-1	+8
6 d	+4	+11	+7	+6	+7	-	-3	-2	-3	-
	-3	-5	-7	-3	-11	-15	+4	0	+8	+12

TABLE II (cont.)

Point	Stresses kgcm^{-2}						Deviation from the prototype values, kgcm^{-2}			
	Proto type	Model tests			Analytical computations		Model tests		Analytical computations	
		plaster	plaster cracked	alkathene	trial-load	independent arches	plaster, cracked	alkathene	trial-load	independent arches
7 d	-7	+5	-	-3	-2	-	-12 b)	-4	-5	-
	-13	-15		-15	-26	-38	+2 b)	+2	+13	+25
8 u	-6	-8	-14	-6	-10	-	+8	0	+4	-
	-29	-23	-26	-24	-16	-22	-3	-5	-13	-7
9 d	-2	+2	-4	+1	+9	-	+2	-3	-11	-
	-16	-11	-9	-7	-18	-24	-7	-9	+2	+8
10 u	-10	-15	-7	-23	-21	-	-3	+13 c)	+11 c)	-
11 d	+4	-6	-4	-7	-15	-	0	+11 c)	+19 c)	-
12 u	-13	-11	-10	-7	-17	-	-3	-6	+4	-
13 d	-10	-13	-11	-11	-19	-	+1	+1	+9	-
14 u	-14	-18	-	-8	-16	-	+4 b)	-6	+2	-
15 d	-25	-34	-28	-20	-21	-	+3	-5	-4	-
16 u	-5	-7	-	-3	-13	-	+2 b)	-2	+8	-
	-26	-25		-18	-16	-22	-1 b)	-8	-10	-4

a) Values obtained without a crack at the heel
b) Values relative to the model without downstream cracks
c) Values greatly influenced by downstream cracks

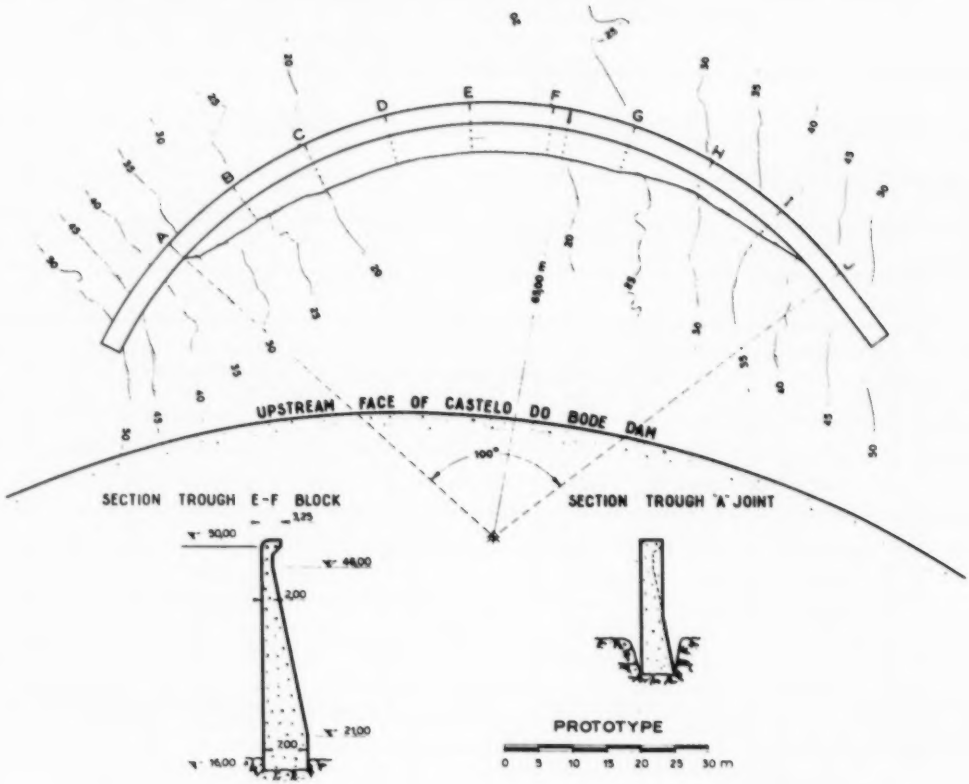

FIG. 1 - CASTELO DO BODE UPSTREAM COFFERDAM - PLAN AND SECTIONS

FIG. 2 - CASTELO DO BODE UPSTREAM COFFERDAM - - VIEW DURING RESERVOIR FILLING. NOTE LEAKAGE AREAS ON DOWNSTREAM FACE

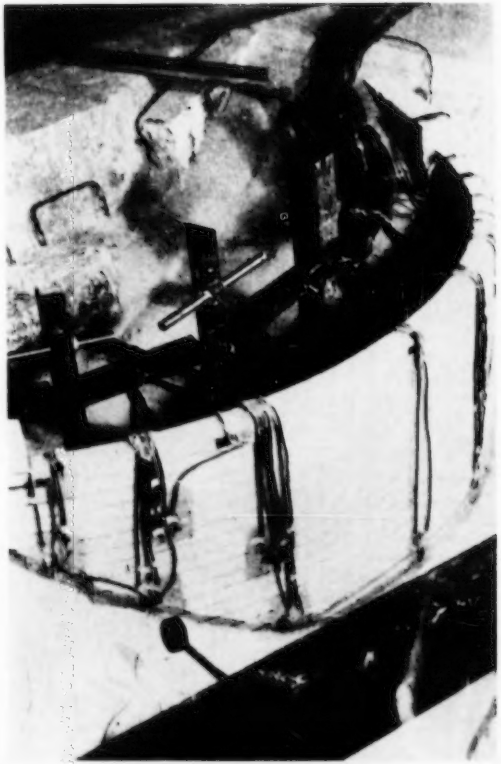

FIG. 3 - PLASTER MODEL, WITH THE ELECTRICAL STRAIN-GAGES

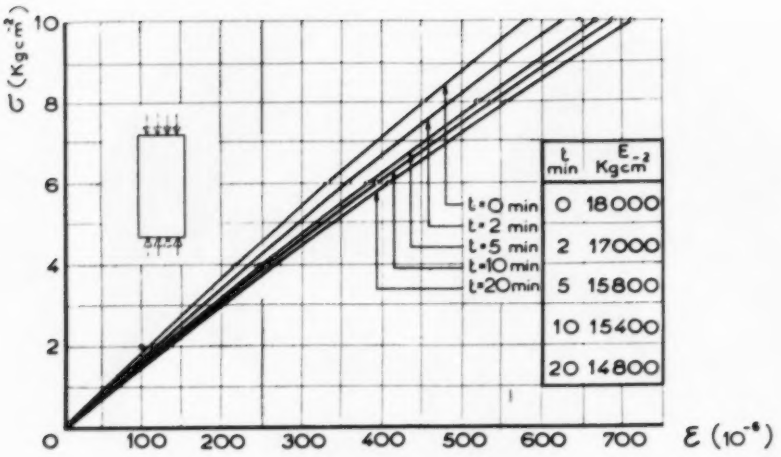

FIG. 4 - MODULUS OF ELASTICITY OF PLASTER FOR DIFFERENT DURATIONS OF LOADING

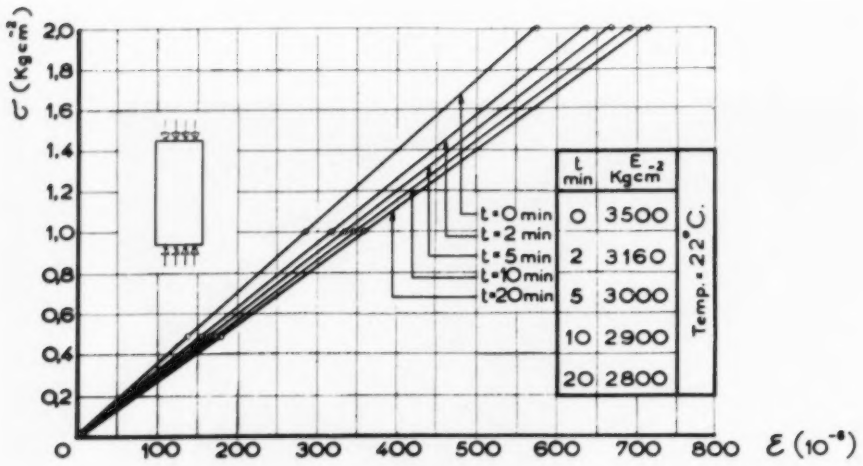

FIG. 5 - MODULUS OF ELASTICITY OF ALKATHENE FOR DIFFERENT DURATIONS OF LOADING, AT 22°C.

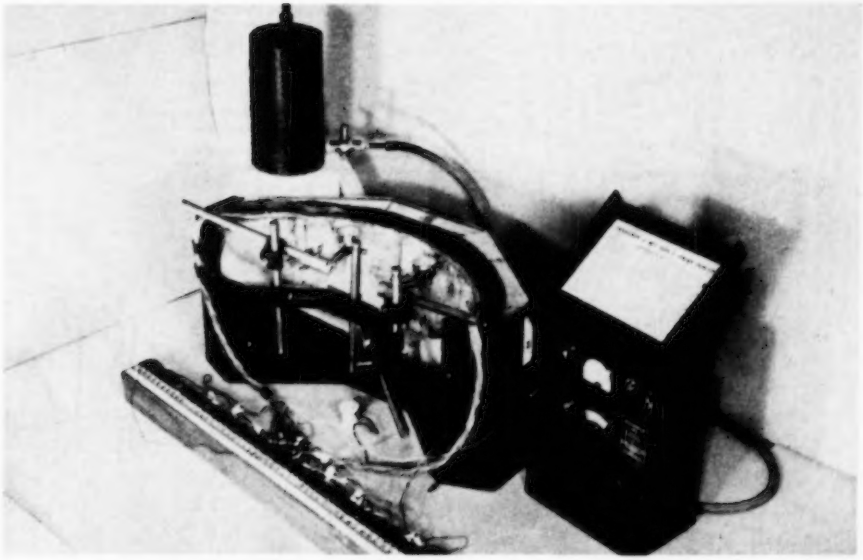

FIG. 6 - ALKATHENE MODEL WITH LOADING DEVICE, READING INSTRUMENT, DEFLECTOMETERS AND STRAIN GAGES

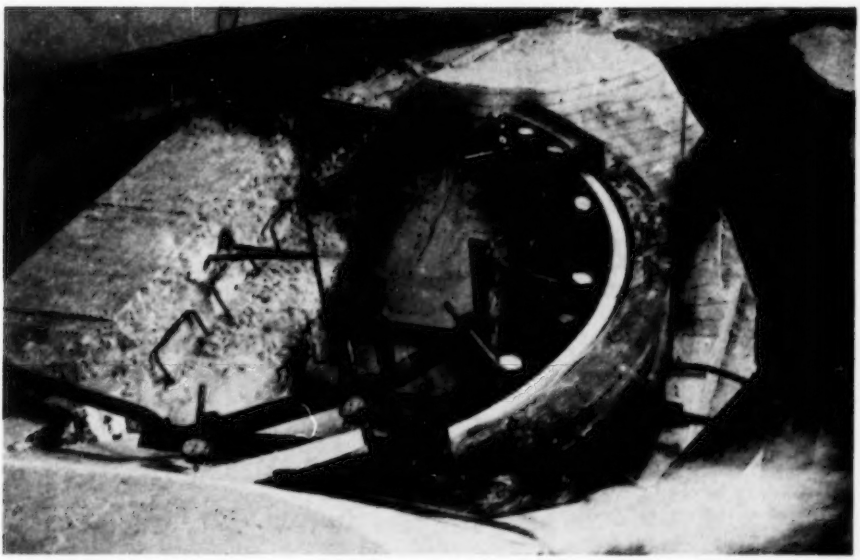

FIG. 7 - PLASTER MODEL, AND DEVICE FOR DEFLECTION MEASUREMENTS

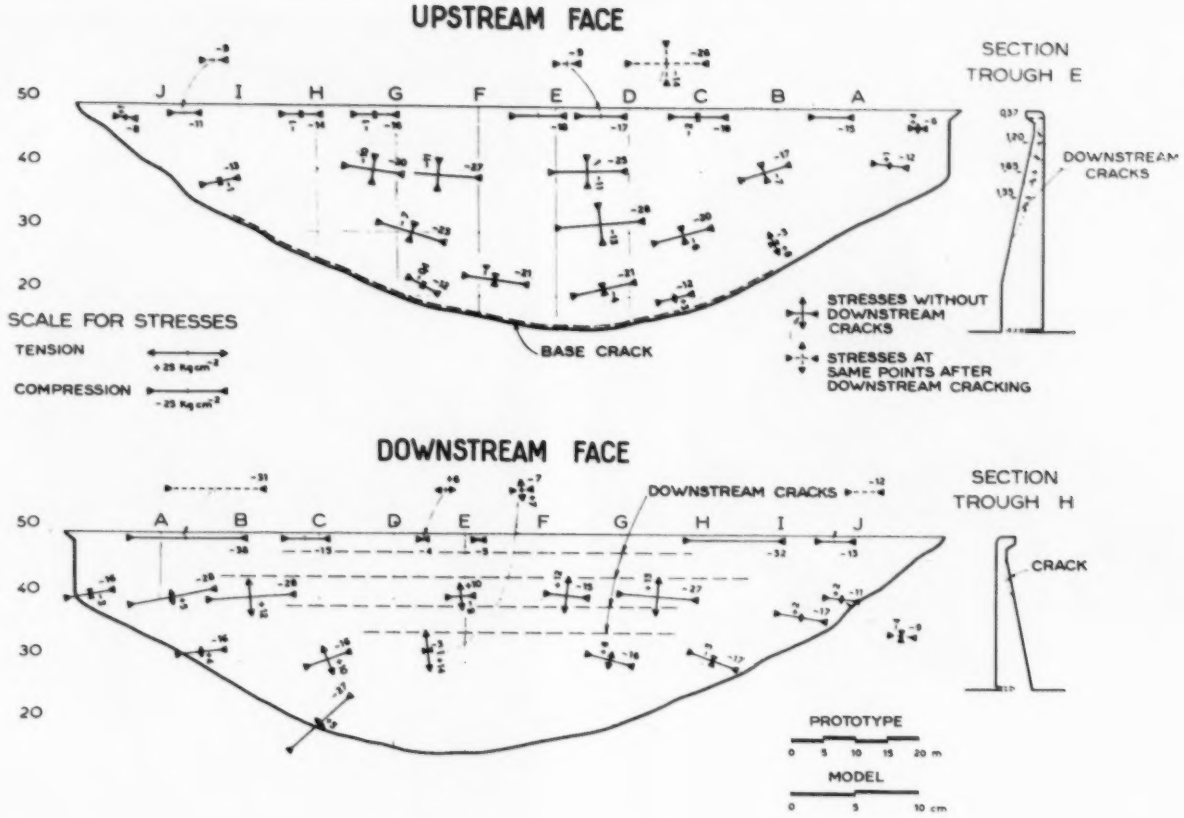

FIG. 8 – STRESSES IN THE PROTOTYPE AS GIVEN BY THE PLASTER MODEL

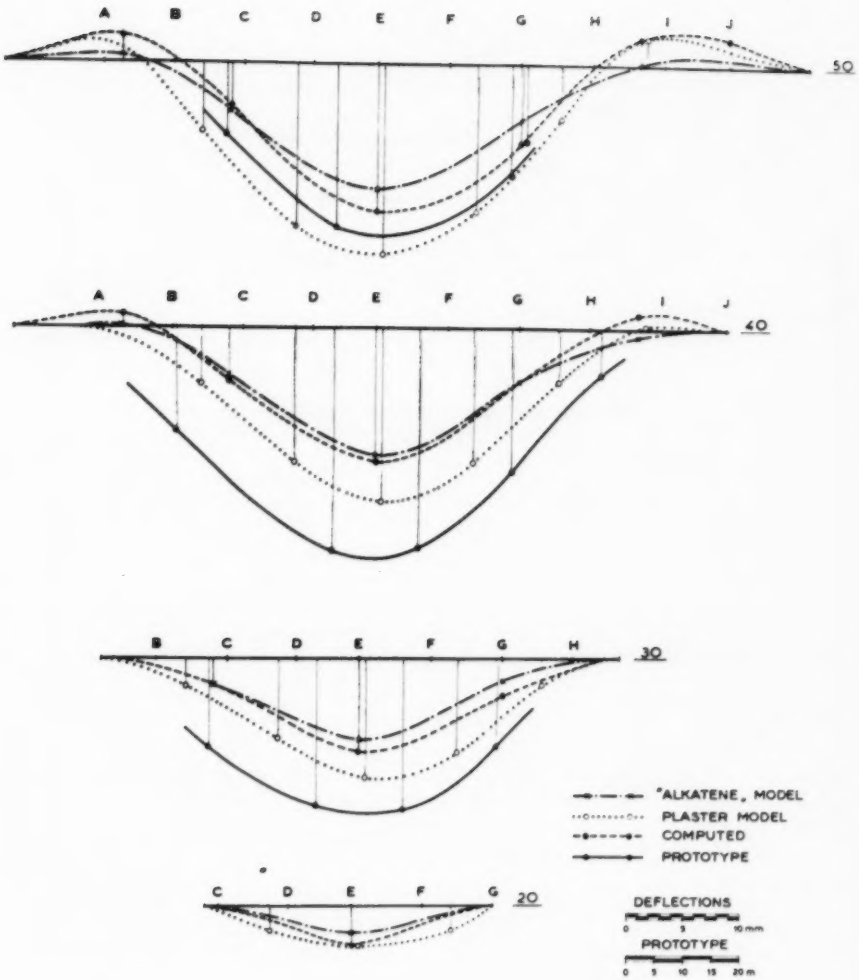

FIG. 9 - COMPARISON OF PROTOTYPE RADIAL DEFLECTIONS AS GIVEN BY MODELS, BY ANALYTICAL CALCULATIONS AND BY PROTOTYPE OBSERVATIONS

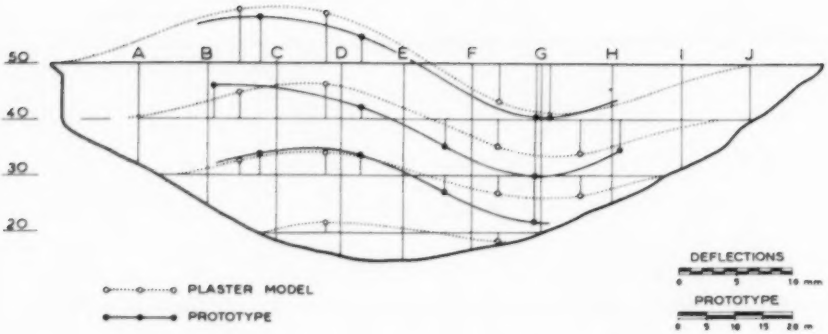

FIG 10 - COMPARISON BETWEEN TANGENCIAL DEFLECTIONS AS GIVEN BY MODEL MEASUREMENTS AND BY PROTOTYPE OBSERVATIONS

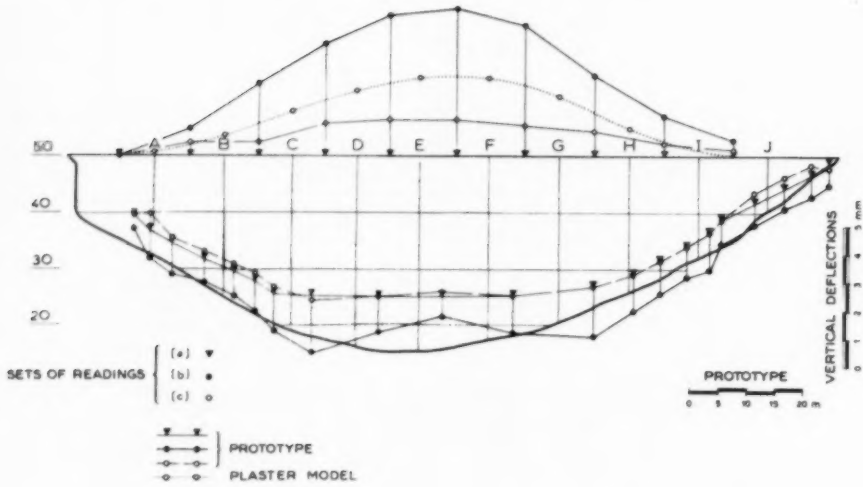

FIG 11 - COMPARISON BETWEEN PROTOTYPE VERTICAL DEFLECTIONS AS GIVEN BY PLASTER MODEL MEASUREMENTS AND BY PROTOTYPE OBSERVATIONS

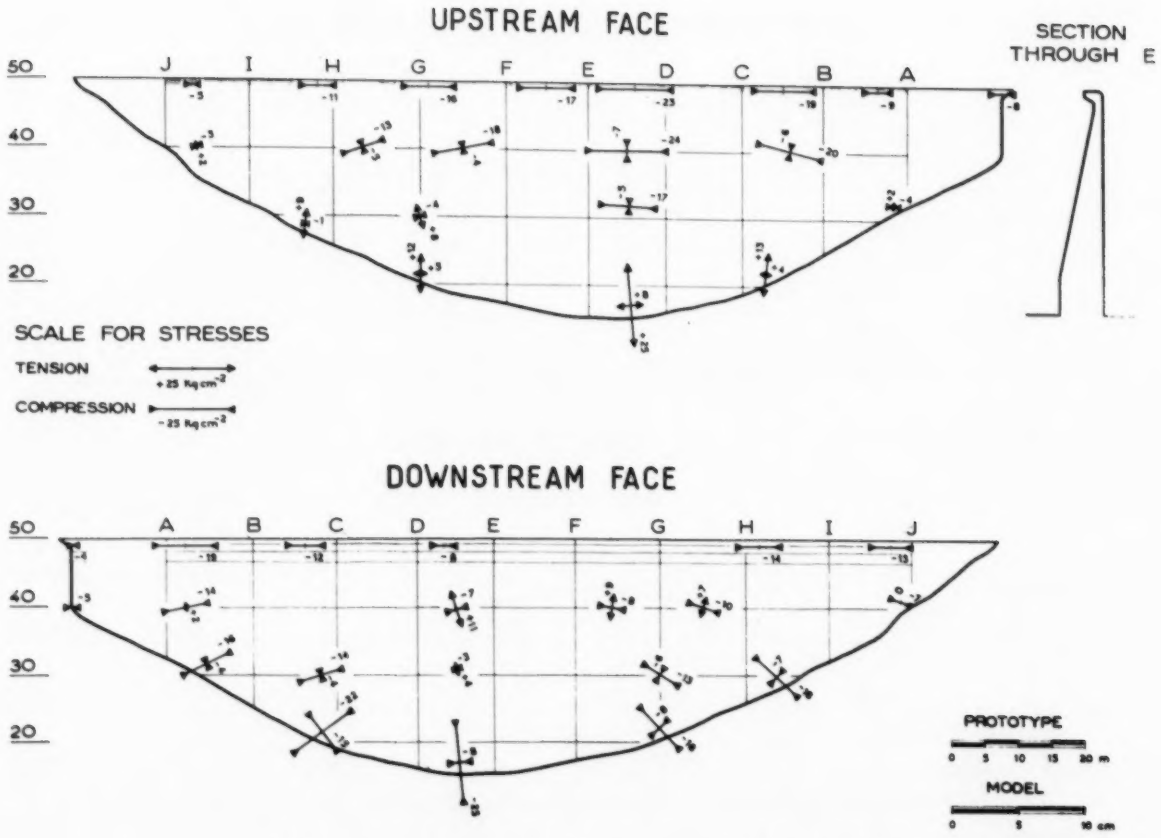

FIG. 12 - PROTOTYPE STRESSES AS GIVEN BY THE ALKATHENE MODEL BEFORE CRACKING

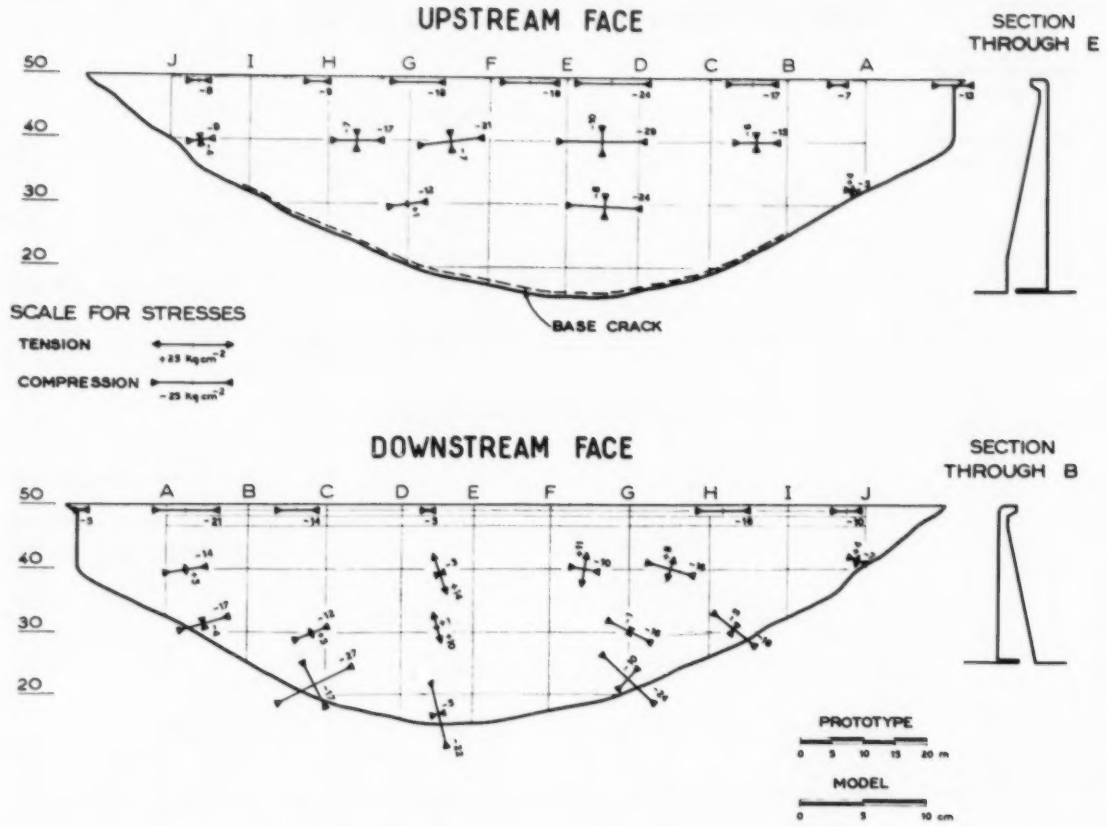

FIG. 13 - PROTOTYPE STRESSES AS GIVEN BY THE ALKATHENE MODEL AFTER CRACKING

CANTILEVERS AND ARCHES CONSIDERED FOR TRIAL-LOAD ANALYSIS

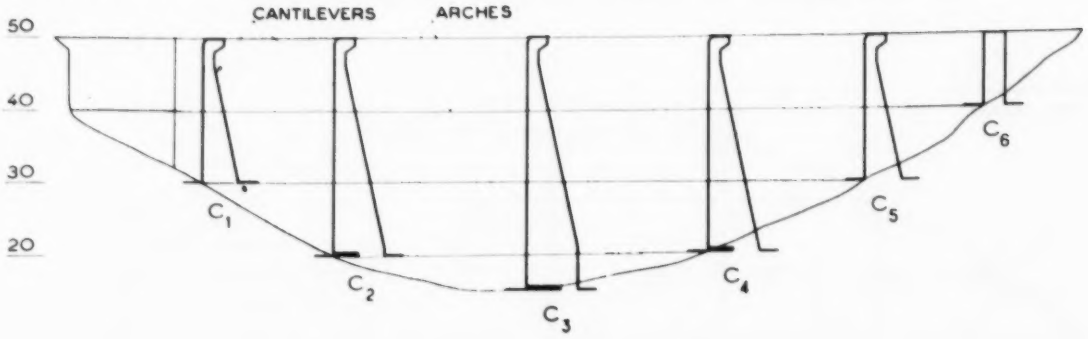

LOAD DISTRIBUTION

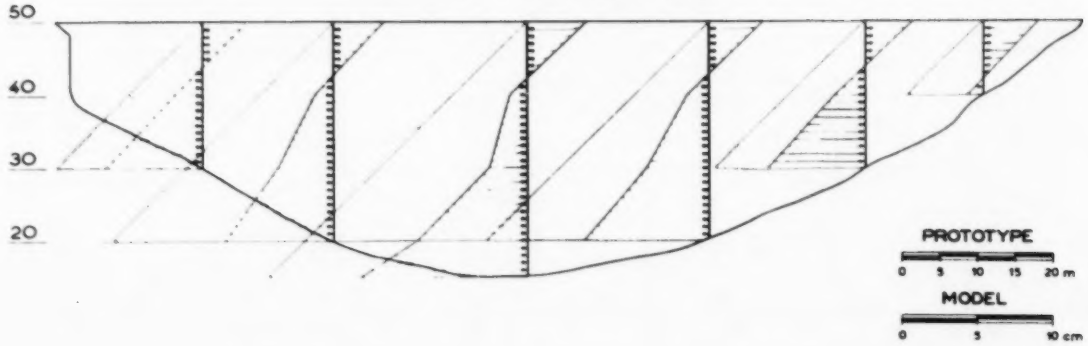

FIG 14 – TRIAL-LOAD ANALYSIS. DISTRIBUTION OF HYDROSTATIC PRESSURE ON ARCHES AND CANTILEVERS

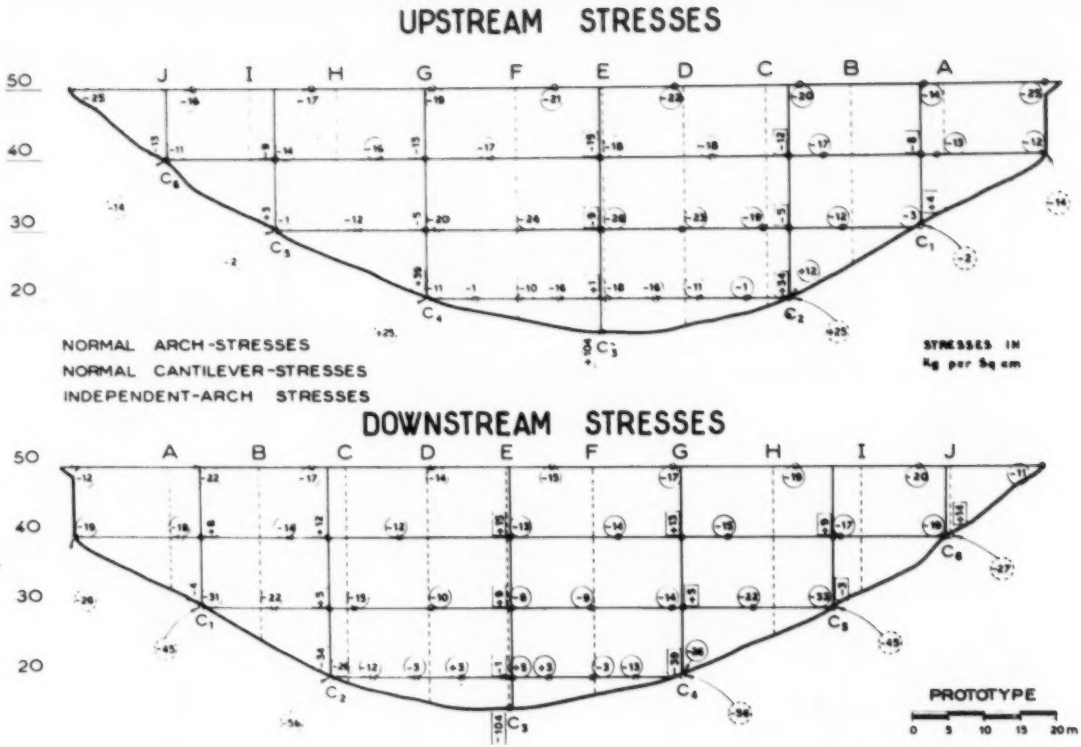

FIG. 15 - PROTOTYPE STRESSES AS GIVEN BY TRIAL-LOAD ANALYSIS

LOCATION OF POINTS OBSERVED BY GEODETIC METHOD BY LEVELLING AND BY MEANS OF CLINOMETER

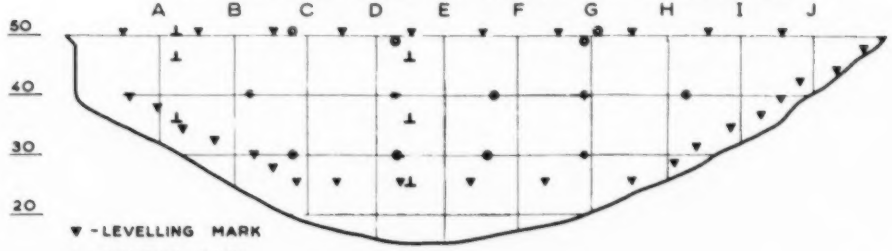

LOCATION OF STRAIN METERS

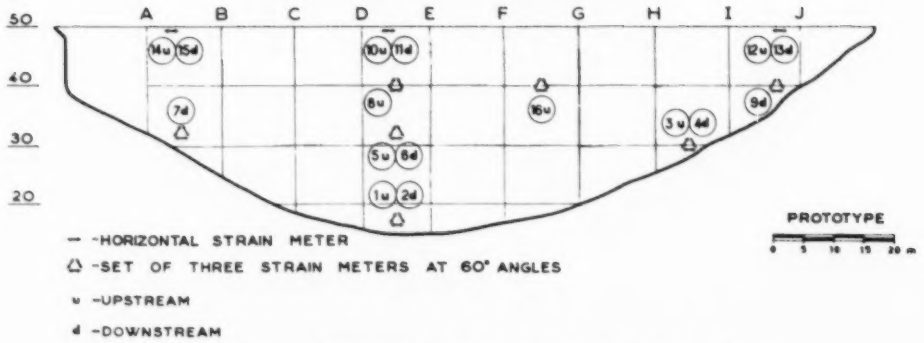

FIG. 16 - LOCATION OF THE POINTS OF THE PROTOTYPE OBSERVED BY THE GEODETIC METHOD, PRECISION LEVELLING, CLINOMETERS AND STRAIN-METERS

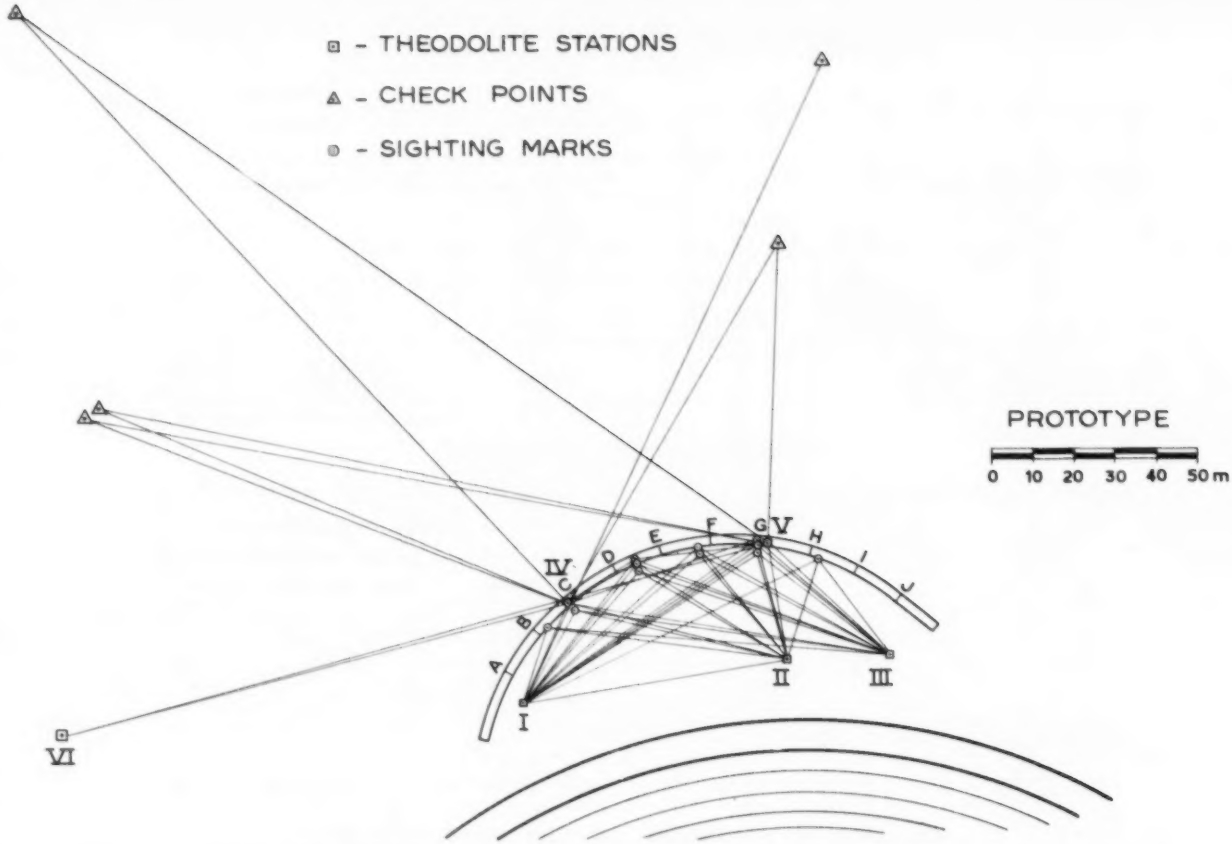

FIG. 17 - SIGHTING DIAGRAMS OF THE PROTOTYPE OBSERVATIONS BY THE GEODETIC AND SLIDE-TARGET METHODS

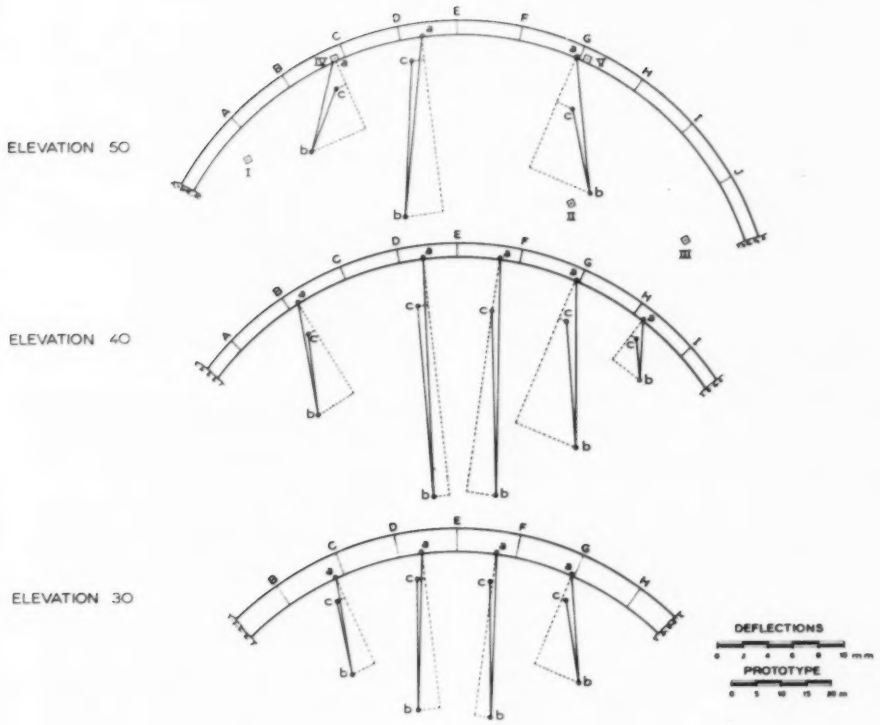

FIG 18 - DEFLECTION TRAJECTORIES OF THE POINTS OF THE PROTOTYPE OBSERVED BY THE GEODETIC METHOD

SLIDE TARGET METHOD

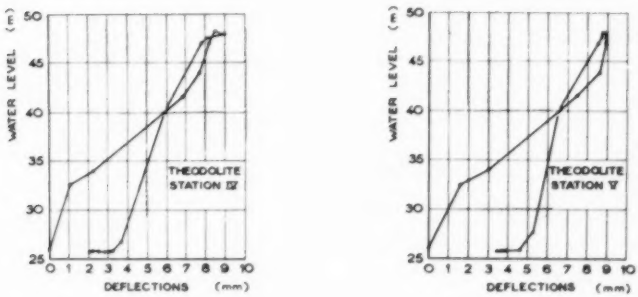

FIG 19 - DISPLACEMENT UNDERGONE BY CROWN MARKS IV AND V AS GIVEN BY THE SLIDE - TARGET METHOD

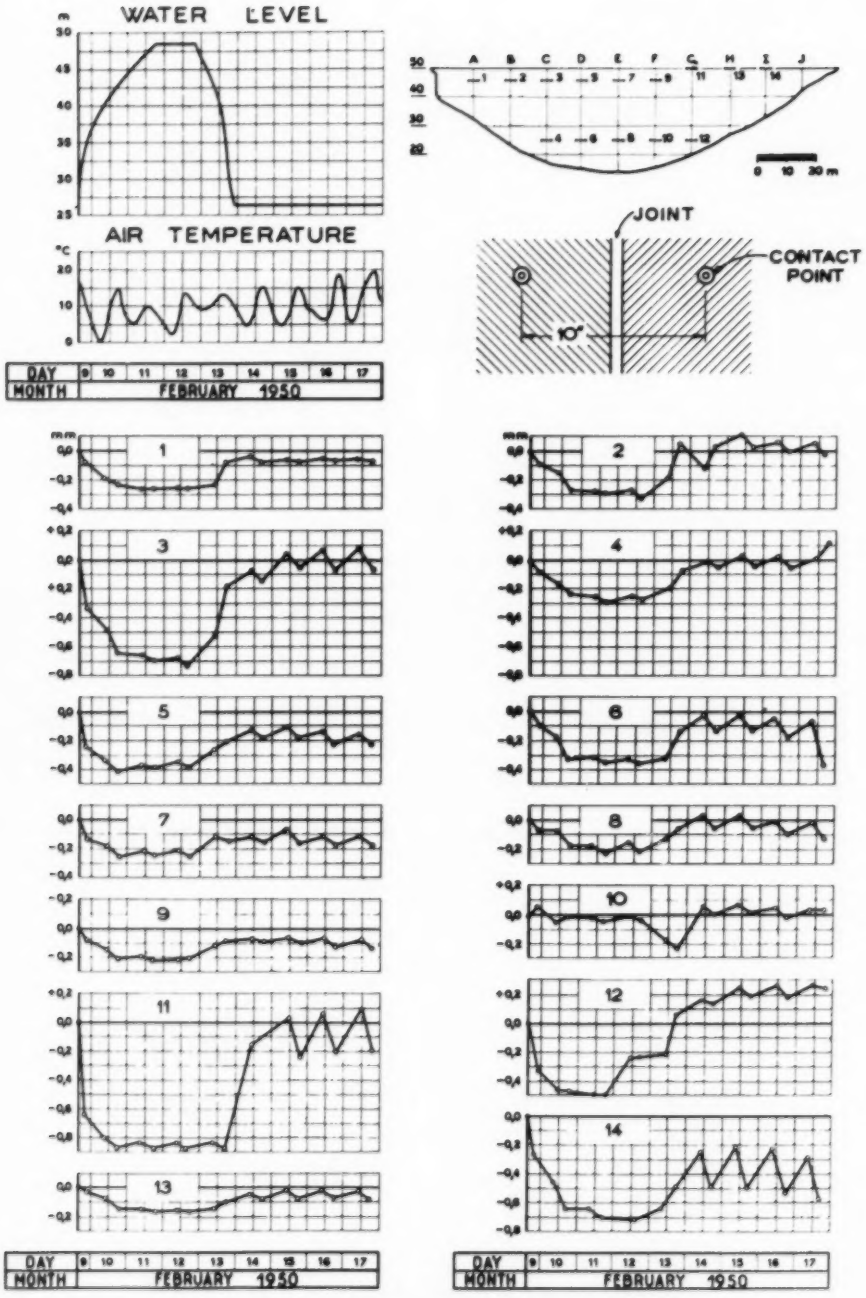

FIG. 20 - JOINT-OPENING DIAGRAM OF THE PROTOTYPE

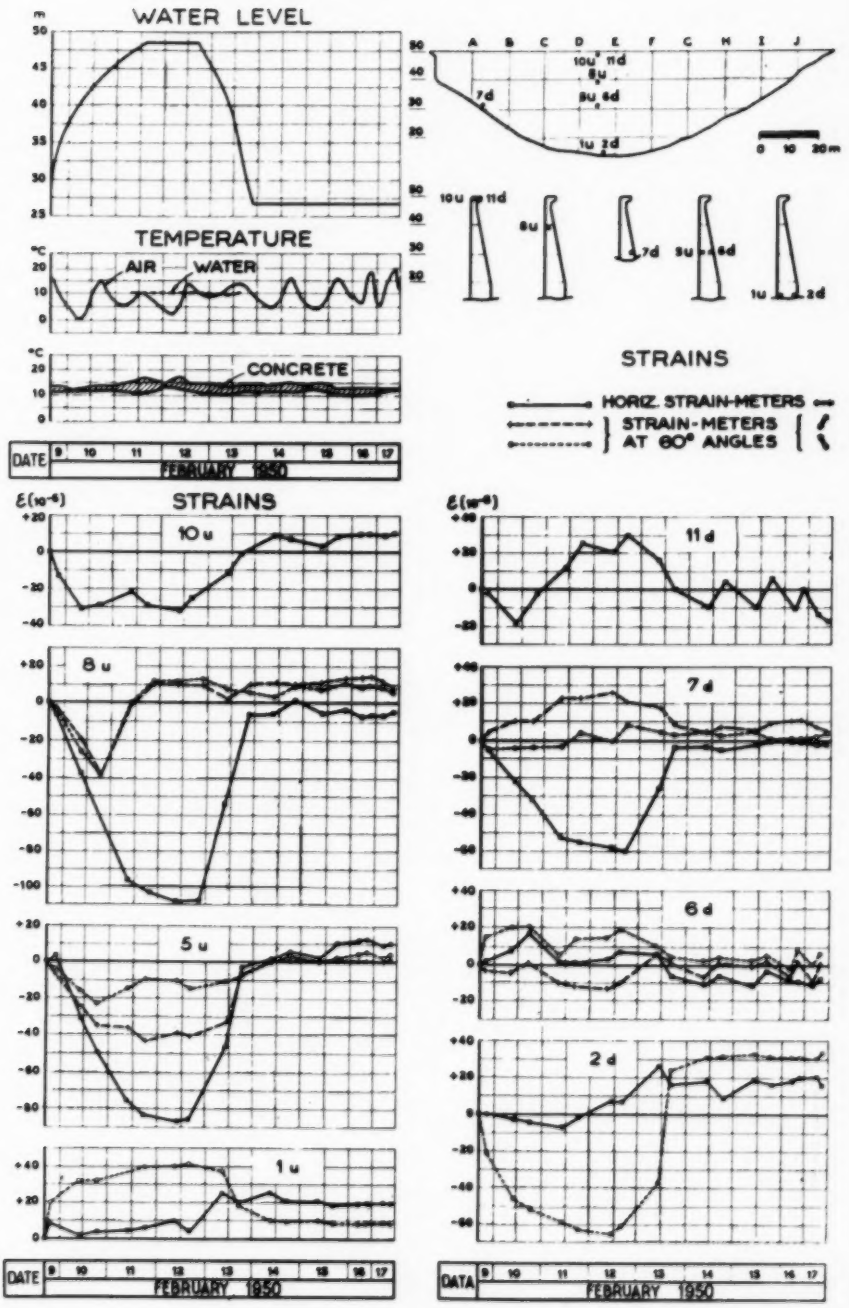

FIG. 21 - DIAGRAM OF STRAINS MEASURED IN THE PROTOTYPE

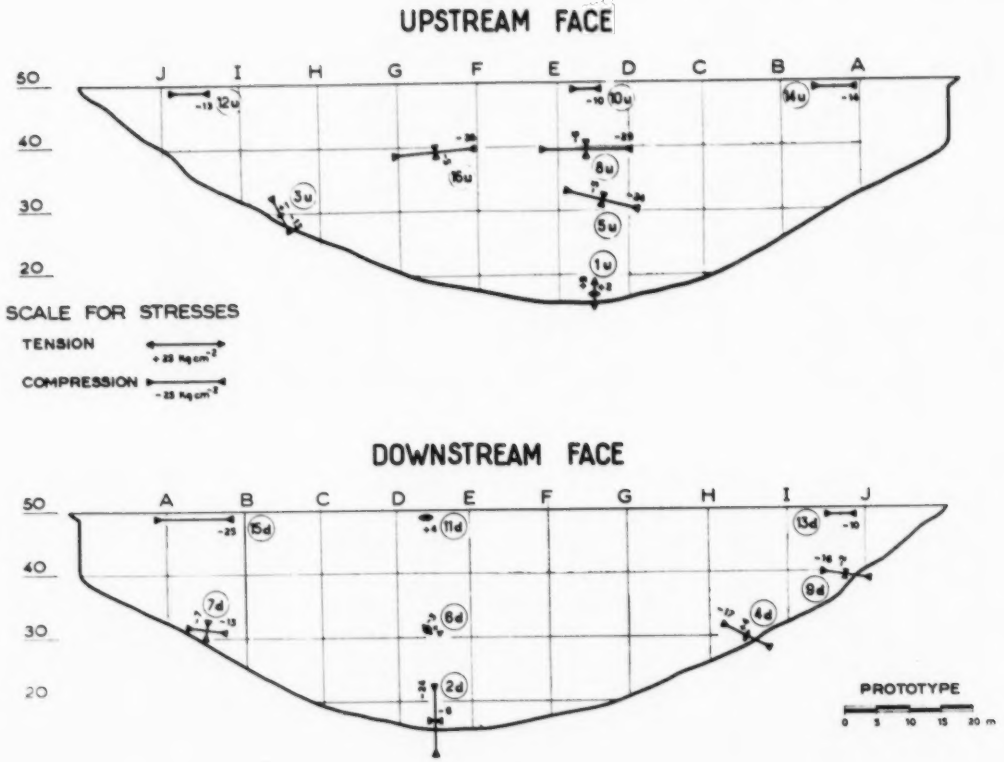

FIG. 22 - PROTOTYPE STRESSES AS DETERMINED FROM PROTOTYPE MEASUREMENTS